Cell

Endoplasmic Reticulum PI(3)P Lipid Binding Targets Malaria Proteins to the Host Cell

Souvik Bhattacharjee,[1,2] Robert V. Stahelin,[3,4] Kaye D. Speicher,[5] David W. Speicher,[5] and Kasturi Haldar[1,2,*]
[1]Center for Rare and Neglected Diseases
[2]Department of Biological Sciences
[3]Department of Chemistry and Biochemistry
University of Notre Dame, Notre Dame, IN 46556, USA
[4]Department of Biochemistry and Molecular Biology, Indiana University School of Medicine, South Bend, South Bend, IN 46617, USA
[5]Center for Systems and Computational Biology and Molecular and Cellular Oncogenesis Program, Wistar Proteomics Core Facility, The Wistar Institute, Philadelphia, PA 19104, USA
*Correspondence: khaldar@nd.edu
DOI 10.1016/j.cell.2011.10.051

SUMMARY

Hundreds of effector proteins of the human malaria parasite *Plasmodium falciparum* constitute a "secretome" carrying a host-targeting (HT) signal, which predicts their export from the intracellular pathogen into the surrounding erythrocyte. Cleavage of the HT signal by a parasite endoplasmic reticulum (ER) protease, plasmepsin V, is the proposed export mechanism. Here, we show that the HT signal facilitates export by recognition of the lipid phosphatidylinositol-3-phosphate (PI(3)P) in the ER, prior to and independent of protease action. Secretome HT signals, including those of major virulence determinants, bind PI(3)P with nanomolar affinity and amino acid specificities displayed by HT-mediated export. PI(3)P-enriched regions are detected within the parasite's ER and colocalize with endogenous HT signal on ER precursors, which also display high-affinity binding to PI(3)P. A related pathogenic oomycete's HT signal export is dependent on PI(3)P binding, without cleavage by plasmepsin V. Thus, PI(3)P in the ER functions in mechanisms of secretion and pathogenesis.

INTRODUCTION

Malaria continues to extract a major toll on human health. The most virulent of human malarias is caused by the protozoan parasite *Plasmodium falciparum*. It is responsible for a million deaths in children each year, largely in sub-Saharan Africa (WHO, 2010). The symptoms and pathologies of disease are caused by blood stage parasites that infect erythrocytes (Miller et al., 2002). The intraerythrocytic parasite resides and proliferates within a parasitophorous vacuolar membrane (PVM; Figure 1). Proteins are exported from the parasite, across the PVM into the cytoplasm and membrane of the erythrocyte to induce changes in transport and membrane properties of the host cell (Haldar and Mohandas, 2007; Maier et al., 2009; Nguitragool et al., 2011). Several hundred *P. falciparum* proteins are predicted to be released into the erythrocyte (Hiller et al., 2004; Marti et al., 2004; Sargeant et al., 2006; van Ooij et al., 2008) including adhesins directly linked to severe and fatal disease pathologies of cerebral malaria and placental malaria (Kyes et al., 2007; Duffy and Fried, 2003).

Parasite proteins destined for the erythrocyte are expected to be first recruited into the endoplasmic reticulum (ER) via an N-terminal signal sequence or a transmembrane domain (Lopez-Estraño et al., 2003). The presence of a consensus host (cell) targeting (HT) or *Plasmodium* export element (PEXEL) signal RxLxE/D/Q downstream of the signal peptide or transmembrane domain is known to export proteins to the erythrocyte (Hiller et al., 2004; Marti et al., 2004; Sargeant et al., 2006; van Ooij et al., 2008). As shown schematically in Figure 1, the HT signal is cleaved in the parasite's ER (Chang et al., 2008; Osborne et al., 2010). In vitro data suggest that cleavage is due to a resident ER protease plasmepsin V (Boddey et al., 2010; Russo et al., 2010) that functions in lieu of signal peptidase to release newly synthesized protein from the ER membrane. Cleavage by plasmepsin V is also proposed to be the mechanism for host targeting (Boddey et al., 2010; Russo et al., 2010), but the underlying mechanisms remain unknown.

The malarial HT signal is related both in sequence and function to the host-targeting signal of another eukaryotic pathogen, the oomycete *Phytophthora infestans*, which infects plant cells and caused the Irish potato famine (Whisson et al., 2007). The *P. infestans* signal is composed of the sequence RxLR…DEER, which if expressed in *P. falciparum*, can target reporter proteins to the host erythrocyte (Bhattacharjee et al., 2006). Conversely malarial HT signal when expressed in *P. infestans* catalyzes protein export to the host plant cell (Dou et al., 2008). In addition, the oomycete signal RxLR…DEER has recently been shown to bind PI(3)P on the surface of eukaryotic cells as a means of penetrating the host (Kale et al., 2010; Figure S1 available online). The

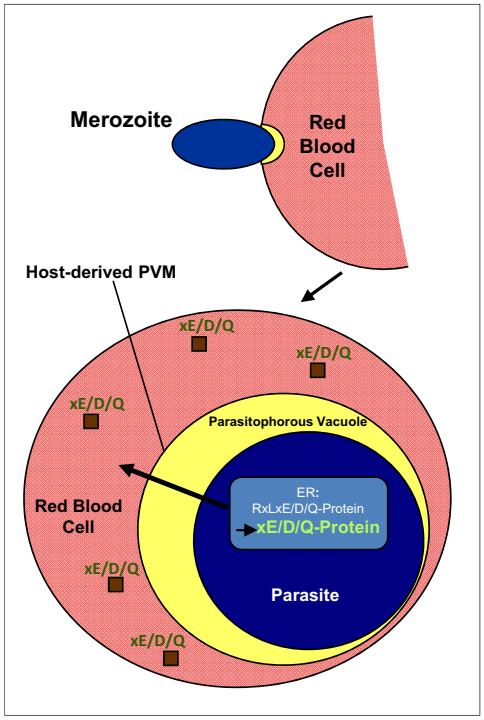

Figure 1. Schematic of Intracellular Infection of *Plasmodium* and Targeting Parasite Proteins to the Host Erythrocyte

A human erythrocyte (pink) infected by *P. falciparum* (blue). Invasion by the extracellular merozoite stage leads to formation of a host derived PVM within which the parasite resides and proliferates. Proteins (brown squares) secreted by the parasite must cross the PVM to reach and mediate virulence and structural changes in the erythrocyte. A consensus motif of RxLxE/D/Q at the N terminus of parasite proteins is proteolytically cleaved after the RxL in the ER, to generate proteins bearing xE/D/Q at their N terminus that are then exported from the ER to the erythrocyte.

binding of this HT signal to PI(3)P was a surprising finding. Polyphosphoinositide binding and binding to the phosphomonoester phosphatidic acid have been attributed to small but cationic rich motifs (McLaughlin et al., 2002; Stace and Ktistakis, 2006). However, to date identified PI(3)P effectors have a well-defined PI(3)P-binding pocket in FYVE or PX domains and generally have at least four points of contact with PI(3)P (Kutateladze, 2010). Although the initial specificity of HT signal binding to PI(3)P was established, the underlying mechanism of binding remains undefined. The significance of HT signal binding to lipid for malarial parasites is unknown, because malarial HT signals are cleaved in the ER and no cell surface PI(3)P was detected on host erythrocytes (Kale et al., 2010). Thus, malarial effector proteins cannot utilize PI(3)P to translocate the PVM into the erythrocyte (Figure 1).

RESULTS

PI(3)P Binds the Malarial HT with Both Affinity and Specificity Linked to Export and Is Detected in the Parasite's ER

To investigate the phosphoinositide (PI) specificity of the HT signal (RLLYE) of *P. falciparum* histidine-rich protein II (PfHRPII), green and red fluorescent protein (GFP and RFP) fusions were used in lipid sedimentation assays (Figures 2A, S2, and Table S2). Clearly, both constructs displayed high selectivity for PI(3)P containing vesicles, whereas mutation of the consensus sequence (ALAYA) or the introduction of a cleaved (YE) sequence significantly reduced PI(3)P binding. To further demonstrate the specific nature of PI(3)P binding, Ins1,3P_2 was added to the lipid sedimentation assay to compete with PI(3)P vesicles for HT binding. In both instances (HT-GFP and HT-RFP), Ins1,3P_2 greatly reduced the amount of HT bound to PI(3)P containing vesicles (Figure S2D). Additionally, HT-GFP was able to compete with the high-affinity PI(3)P binding PX domain of p40-phox and displace p40-phox-PX from PI(3)P vesicles in a concentration-dependent manner (Figure 2B).

A lack of quantitative information on the affinity of PI(3)P binding by HT-targeting signals of oomycete/malaria, precludes understanding their relative mechanism of action. We therefore used surface plasmon resonance (SPR) and, as shown in Figures 2C–2E, discovered a high-affinity interaction between the HT signal of PfHRPII and PI(3)P vesicles (36 nM). This was completely abolished by mutation ALAYA ($K_d > 5\ \mu M$). The mutation ALLYE ($K_d > 5\ \mu M$) also abrogated PI(3)P binding, whereas RLAYE and RLLYA reduced binding by 23- and 7-fold, respectively. The relative contribution of R, L and E residues in the HT signal to PI(3)P binding correlated with their relative utilization in the host targeting logo (Figure 2E), suggesting lipid binding and protein export may be linked. Additional HT signals from the major virulence determinant *P. falciparum* erythrocyte membrane protein 1 (PfEMP1) and other parasite effectors known to be targeted into the host erythrocyte, also bound PI(3)P vesicles with nanomolar affinity ranging from 20 to 110 nM. Mutation of R/K with alanine decreased binding by at least 20-fold (Figure 2E), and, in most cases, binding to PI(3)P was not detectable, suggesting that HT signals of multiple, important malarial effector proteins bind PI(3)P. Together these data led us to consider that PI(3)P binding may be a generalized property of a wide range of malaria secretome effectors exported to the erythrocyte.

However, PI(3)P is known to be a cytoplasmic lipid in cells. To bind the HT signal on newly synthesized parasite effectors exported to the erythrocyte, it must be present in the lumen of parasite's secretory pathway and act prior to processing by plasmepsin V in the ER. To the best of our knowledge, there are no reports of the presence of PI(3)P within the secretory pathway of cells. Thus, to investigate this possibility in the malarial secretory pathway, we expressed a secretory fusion of monomeric Cherry (mCherry) and the FYVE domain of early endosomal antigen 1 (EEA1), a protein with nanomolar affinity for PI(3)P (and is widely used to detect the location of PI(3)P in cells (Lee et al., 2005). As shown in Figure 3A, all of the cell associated red fluorescence is detected in punctate regions in a perinuclear location (top), ascribed to a single fusion protein of the expected size (Figure 3B) and recruited to the secretory pathway (as proven by cleavage of the signal sequence, Figure 3C). A point mutation R1374A in the FYVE region of EEA1, known to abrogate PI(3)P binding when introduced into the mCherry fusion, redistributed red fluorescence to the parasite periphery (Figure 3A, bottom), and was released into the supernatant when the red

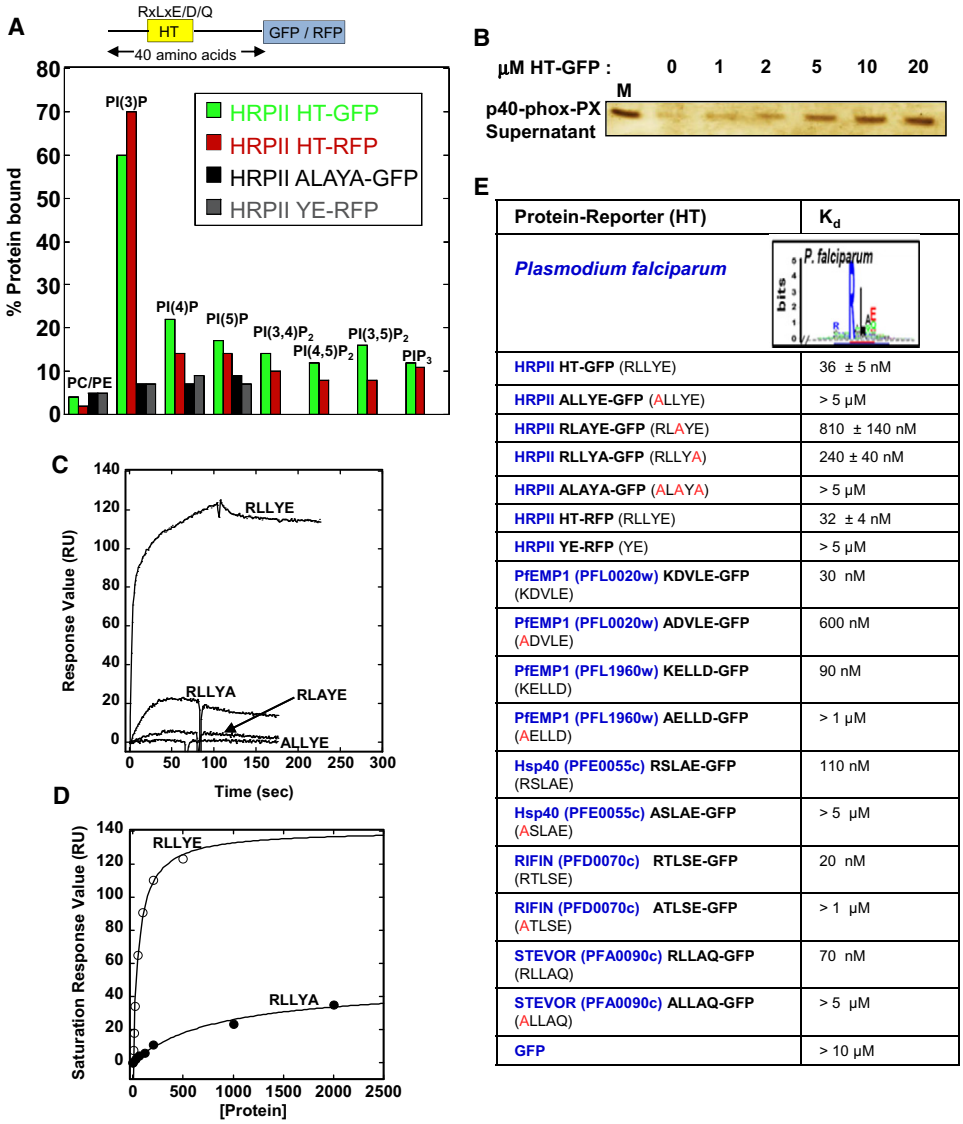

E

Protein-Reporter (HT)	K_d
Plasmodium falciparum	
HRPII HT-GFP (RLLYE)	36 ± 5 nM
HRPII ALLYE-GFP (ALLYE)	> 5 µM
HRPII RLAYE-GFP (RLAYE)	810 ± 140 nM
HRPII RLLYA-GFP (RLLYA)	240 ± 40 nM
HRPII ALAYA-GFP (ALAYA)	> 5 µM
HRPII HT-RFP (RLLYE)	32 ± 4 nM
HRPII YE-RFP (YE)	> 5 µM
PfEMP1 (PFL0020w) KDVLE-GFP (KDVLE)	30 nM
PfEMP1 (PFL0020w) ADVLE-GFP (ADVLE)	600 nM
PfEMP1 (PFL1960w) KELLD-GFP (KELLD)	90 nM
PfEMP1 (PFL1960w) AELLD-GFP (AELLD)	> 1 µM
Hsp40 (PFE0055c) RSLAE-GFP (RSLAE)	110 nM
Hsp40 (PFE0055c) ASLAE-GFP (ASLAE)	> 5 µM
RIFIN (PFD0070c) RTLSE-GFP (RTLSE)	20 nM
RIFIN (PFD0070c) ATLSE-GFP (ATLSE)	> 1 µM
STEVOR (PFA0090c) RLLAQ-GFP (RLLAQ)	70 nM
STEVOR (PFA0090c) ALLAQ-GFP (ALLAQ)	> 5 µM
GFP	> 10 µM

Figure 2. Lipid Binding Properties of HT Signals

(A) Summary of quantitative lipid binding specificity of PfHRPII: HT-GFP, HT-RFP, ALAYA-GFP, and YE-RFP, based on lipid pull down data shown in Figure S2. All proteins (recombinants purified from *E. coli*) contain the HT motif (RxLxE) and flanking sequences (that together comprise the vacuolar translocation sequence), as shown in the schematic. Sequence information is in Table S2.

(B) Competition assay between HT-GFP and the p40-phox-PX domain. p40-phox-PX (5 µM) was incubated with 1 mM PI(3)P containing vesicles, and HT-GFP was added at increasing concentrations from 0 to 20 µM. After 20 min, the supernatant fraction was resolved using SDS-PAGE following centrifugation. M indicates total protein loaded into each reaction.

(C) SPR analysis demonstrates quantitative lipid binding of HT/RLLYE-GFP, ALLYE-GFP, RLAYE-GFP, and RLLYA-GFP for PI(3)P containing vesicles. One micromolar of each construct was injected over a POPC:POPE:PI(3)P (75:20:5) surface at 30 µl/min using POPC:POPE (80:20) as a control. The control response was subtracted from each active surface to yield the displayed sensorgrams.

(D) Equilibrium SPR binding analysis of HT/RLLYE-GFP (open circles) and RLLYA-GFP (filled circles). To determine K_d values, R_{eq} values were plotted versus [P], and the K_d value was determined by a nonlinear least-squares analysis of the binding isotherm using the following equation: $R_{eq} = R_{max}/(1 + K_d/P_0)$. For proteins with weak affinity, dilutions were made up to 10 µM to probe for lipid binding. If no binding was detected this allowed us to estimate the K_d value to be greater than the highest protein concentration used for respective lipid vesicle.

(E) K_d values determined for each recombinant protein using the methods pictured and described in (D). Sequence logo is derived from HT signal of *P. falciparum* secretory proteins. Amino acids are represented by one-letter abbreviations and color-coded as follows: blue, basic; red, acidic; black, hydrophobic; and green, polar. Height of amino acids indicates their frequency at that position. Also see Table S2.

cell and PVM were permeabilized with saponin (Figure 3D), consistent with default secretion into the parasitophorous vacuole (PV). A secretory fusion of a second PI(3)P binding protein (p40-phox-PX) also showed perinuclear, punctate distribution (Figure S3A), whereas a single point mutant p40-phox^{R58Q} that abrogates PI(3)P binding is secreted to the PV (Figures S3A

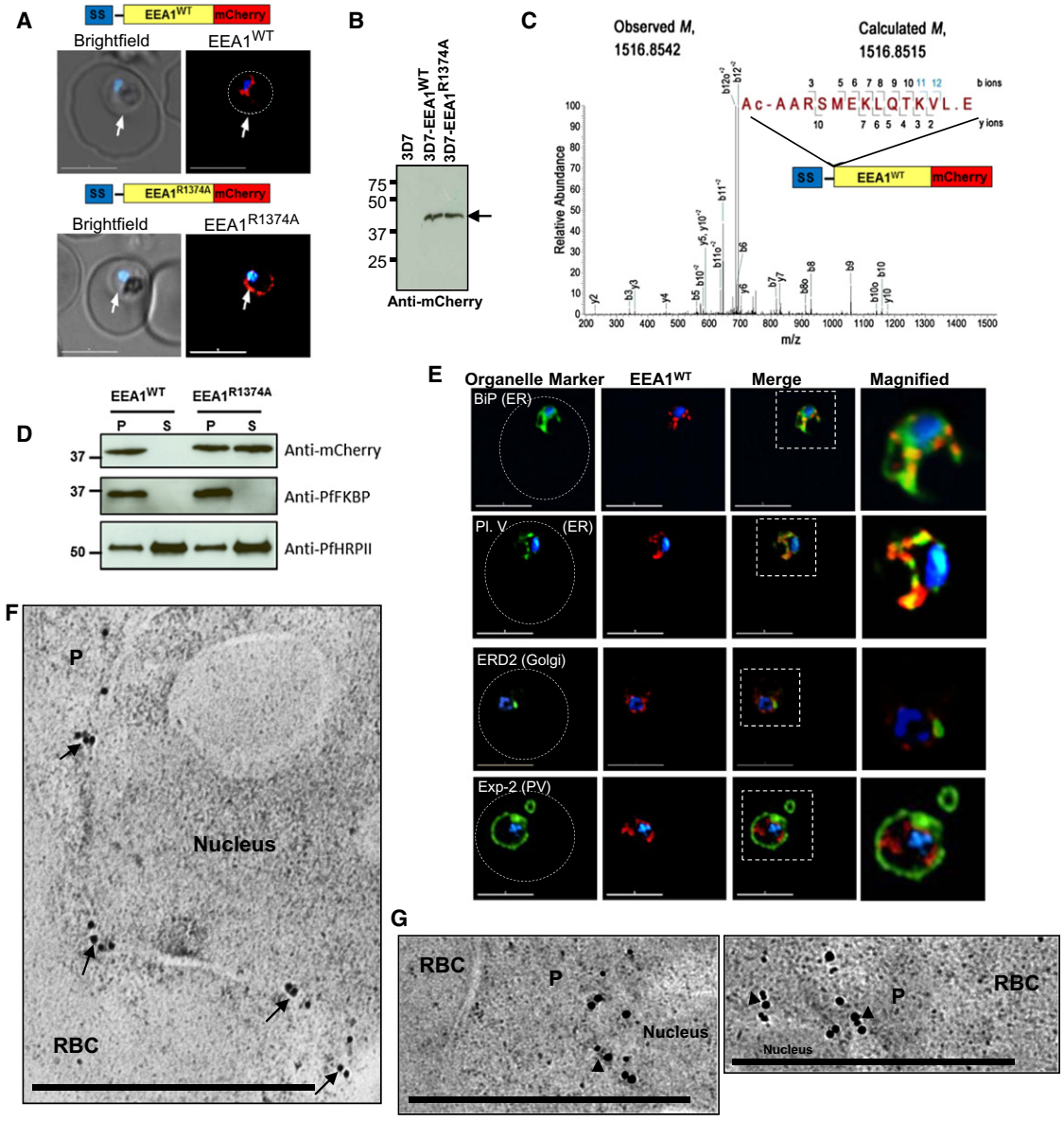

Figure 3. PI(3)P Is Detected in *P. falciparum* Endoplasmic Reticulum

(A) Live *P. falciparum*-infected erythrocytes expressing the FYVE domain of EEA1 as a mCherry fusion recruited to the secretory pathway via an ER-type signal sequence. The wild-type FYVE domain of EEA1 ($EEA1^{WT}$), which binds PI(3)P with nanomolar affinity exhibits perinuclear staining (top). The point mutant FYVE domain of EEA1 ($EEA1^{R1374A}$) that fails to bind PI(3)P shows peripheral staining expected for proteins undergoing default secretion to the PV (bottom). Left panels, bright-field images with Hoechst 33342 nuclear staining (blue); right panels, fluorescence images. Dotted lines in the top panel and arrows (both panels) indicate the location of the PV. Scale bars, 5 μm. Also see Figure S3A.

(B) Western blot of nontransfected 3D7 and transgenic parasites expressing $EEA1^{WT}$ or $EEA1^{R1374A}$ fused to mCherry. A single band at 42 kDa was detected (arrow) for each fusion. Molecular weight standards in kilodaltons are shown in the left.

(C) The ER-type signal sequence (SS) of $EEA1^{WT}$ is cleaved confirming recruitment of $EEA1^{WT}$ to the secretory pathway. $EEA1^{WT}$-mCherry, purified from parasites was digested with AspN and analyzed by LC-MS/MS. Mass spectra revealed that the most N-terminal peptide is Ac-AARSMEKLQTKVL.E, suggesting efficient cleavage of the signal sequence by signal peptidase. Ac- indicates acetylation on N-terminal alanine. Observed b and y ions are shown on the peptide sequence and the MS/MS spectra with neutral loss of water indicated by "o," +1 ions shown in black and +2 ions shown in blue on the peptide sequence. When multiple forms (different charge states or water loss) of an ion were observed, only one form is indicated on the peptide sequence. The observed and calculated masses (M+H) are 1516.8542 and 1516.8515, respectively, indicating a 1.8 ppm mass error.

(D) Saponin lysis of transgenic parasites expressing secretory $EEA1^{WT}$ and $EEA1^{R1374A}$. Western blots (top row) indicate that $EEA1^{R1374A}$ is detected into the supernatant (S) and thus released into the PV, whereas $EEA1^{WT}$ is retained within the parasite pellet (P). The parasite cytosolic protein PfFKBP (middle row) is not released, confirming parasite integrity. PfHRPII (bottom row) exported to the erythrocyte and $EEA1^{R1374A}$ released in the PV are also detected in parasite pellets (P) because they are continuously synthesized there. Molecular weight standards in kilodaltons are shown in the left. Also see Figure S3B.

and S3B), again suggesting that PI(3)P is present in highly localized secretory regions within the parasite. These PI(3)P enriched regions appear to reside in a subset of structures labeled by BiP, a resident ER protein (Figures 3E and S3C) and also show overlap with plasmepsin V (another parasite ER protein) but their distribution appears to be distinct from that of the early Golgi marker (ERD2) and a protein of the PVM surrounding the intracellular parasite (Figure 3E). This suggested that PI(3)P-enriched regions are likely to be present early in the secretory pathway, in the ER, but are not concentrated in the Golgi or periphery of the parasite. Immunoelectron microscopy studies revealed that PI(3)P is detected in regions of reticular membranes closely apposed to the nucleus (Figures 3F and S3D), and localizes to perinuclear, tubovesicular structures containing the ER marker, BiP, confirming its localization in the ER (Figure 3G).

An Endogenous, ER Form of PfHRPII Protein Containing the HT Signal Recognizes PI(3)P prior to Cleavage by Plasmepsin V

Since PI(3)P is found in the malarial ER and displays nanomolar affinity for HT signal in in vitro assays, we investigated whether the HT signal on the endogenous ER form of an effector protein is associated with PI(3)P. Since plasmepsin V cleaves to separate the sequences upstream of the HT signal from the rest of the effector protein, we generated antibodies to recognize the uncleaved precursor protein form but not the processed mature protein.

As shown in Figures 4A and 4B, antibodies to the pre-HT region of PfHRPII protein (also called anti-(pre-HT)) recognized recombinant protein produced in *Escherichia coli* from constructs 1-4, but not 5-6 that lacked pre-HT region. In immunolocalization assays, pre-HT antibodies recognize protein only within the parasite (Figure 4C, top). In contrast, antibodies to sequences (YETQAHVDDVHHAHHADV) downstream of the HT signal, also called post-HT-antibodies, detect PfHRPII exported to the erythrocyte as well as within the parasite (Figure 4C, bottom). In western blots, pre-HT antibodies recognized a single, endogenous protein band above the 50 kDa marker (asterisk in Figure 4D, left) restricted to the parasite pellet upon saponin treatment. In contrast, post-HT antibodies also recognize a second exported form released into the supernatant (arrowhead in Figure 4D, right). These data confirm the presence of a precursor PfHRPII (pPfHRPII) protein containing the HT motif located within the parasite. Further, pPfHRPII is in the ER and serves as its marker, since plasmepsin V (which cleaves the HT motif of pPfHRPII) resides in the ER.

It should be noted that these experiments were undertaken with parasites ~12 hr in the intraerythrocytic infection cycle, when PfHRPII is maximally synthesized, to facilitate detection of endogenous precursors. Endogenous pPfHRPII was immunopurified using pre-HT antibodies, and found to contain ~10-fold higher levels of PI(3)P relative to complexes immunopurified with post-HT antibodies, on a per mole protein basis (Figures 4E and S4). The extent of concentration was comparable to the level of PI(3)P binding observed with secretory EEA1^{WT} relative to binding by the EEA1^{R1374A} mutant (Figures 4F and S4). SPR analyses confirmed that the endogenous HT-signal bearing precursor displayed high affinity for PI(3)P (Figure 4G). The interaction of the pPfHRPII with PI(3)P was specific since the interaction with a second phosphoinositide, PI(4)P was undetectable (Figure 4H). Together, these biochemical analyses firmly establish that endogenous HT signal can be detected on protein prior to cleavage by plasmepsin V and thus resident in the ER. This ER precursor binds PI(3)P with nanomolar affinity. Major sites of PI(3)P/EEA1^{WT} accumulation, showed partial coassociation with pPfHRPII in indirect immunofluorescence assays (Figure 4I). It should be noted that in cells endogenous pPfHRPII will compete with (potentially) hundreds of additional effectors for PI(3)P in the ER. Nonetheless colocalization of pPfHRPII and EEA1^{WT} was also seen in perinuclear regions by immunoelectron microscopy (Figure 4J), strongly supporting that pPfHRPII and PI(3)P come together in the ER (or ER-derived membranes).

HT Signal-Dependent and -Independent Export of Parasite Proteins to the Host Erythrocyte in the Absence of Cleavage by Plasmepsin V

In the parasite ER, PI(3)P binding by the malarial HT signal must precede HT signal cleavage by plasmepsin V. However, since the relative importance of the individual residues in PI(3)P binding are the same as those for protease cleavage, it is difficult to resolve the relative importance of each to host targeting. To do so, we turned to the oomycete HT signal that we have previously shown to mediate protein export from the parasite to the host erythrocyte (Bhattacharjee et al., 2006). Since the susceptibility of the RQLR…DEER motif to the malarial protease was unknown, we engineered a signal peptidase cleavage site by insertion of AAAA, immediately after the signal sequence and prior to the HT motif of the oomycete *Phytophthora infestans* effector protein Nuk10, fused to GFP (see Extended Experimental Procedures). Expression of this construct in *P. falciparum*, resulted in export of GFP from the malaria parasite to the erythrocyte (Figure 5A, top, and Figure 5B), which was blocked by mutation of the RQLR motif (Figure 5A, bottom).

To investigate the relative contribution of plasmepsin V cleavage to export, we undertook mass spectrometric analysis of purified Nuk10-WT-GFP and mutant. Analysis of the most

(E) Localization of EEA1^{WT}-mCherry as a marker for PI(3)P in the parasite ER. Transgenic parasites were fixed, permeabilized and probed with anti-mCherry as well as antibodies to endogenous *P. falciparum* markers (green) of the ER, like BIP (top row) and plasmepsin V (Pl. V, second row); a marker of the Golgi (ERD2, third row) or the PVM (Exp-2, bottom row). EEA1^{WT} (red) is seen in punctuate 'spots' within the ER. Dotted circles show location of red cell membrane. Dotted squares show regions magnified in the right panels. Parasite nuclei were stained with Hoechst 33342 (blue). Scale bars, 5 μm. Also see Figure S3C.

(F and G) Immunoelectronmicroscopy showing localization of EEA1^{WT}-mCherry in perinuclear membranes and its coassociation with the ER marker BiP. (F) Thin sections, probed with anti-mCherry and secondary antibody gold conjugates (10 nm) show label concentrated in membrane regions emerging from reticular membrane apposed to the nucleus (arrows), consistent with localization in the ER. (G) Thin sections probed for EEA1^{WT}-mCherry (10 nm gold) and BiP (15 nm gold). Arrowheads show closed localization of BiP and EEA1^{WT} site. RBC, red blood cells; P, parasite. Scale bar, 0.5 μm. Control data for immunogold labeling is shown in Figure S3D.

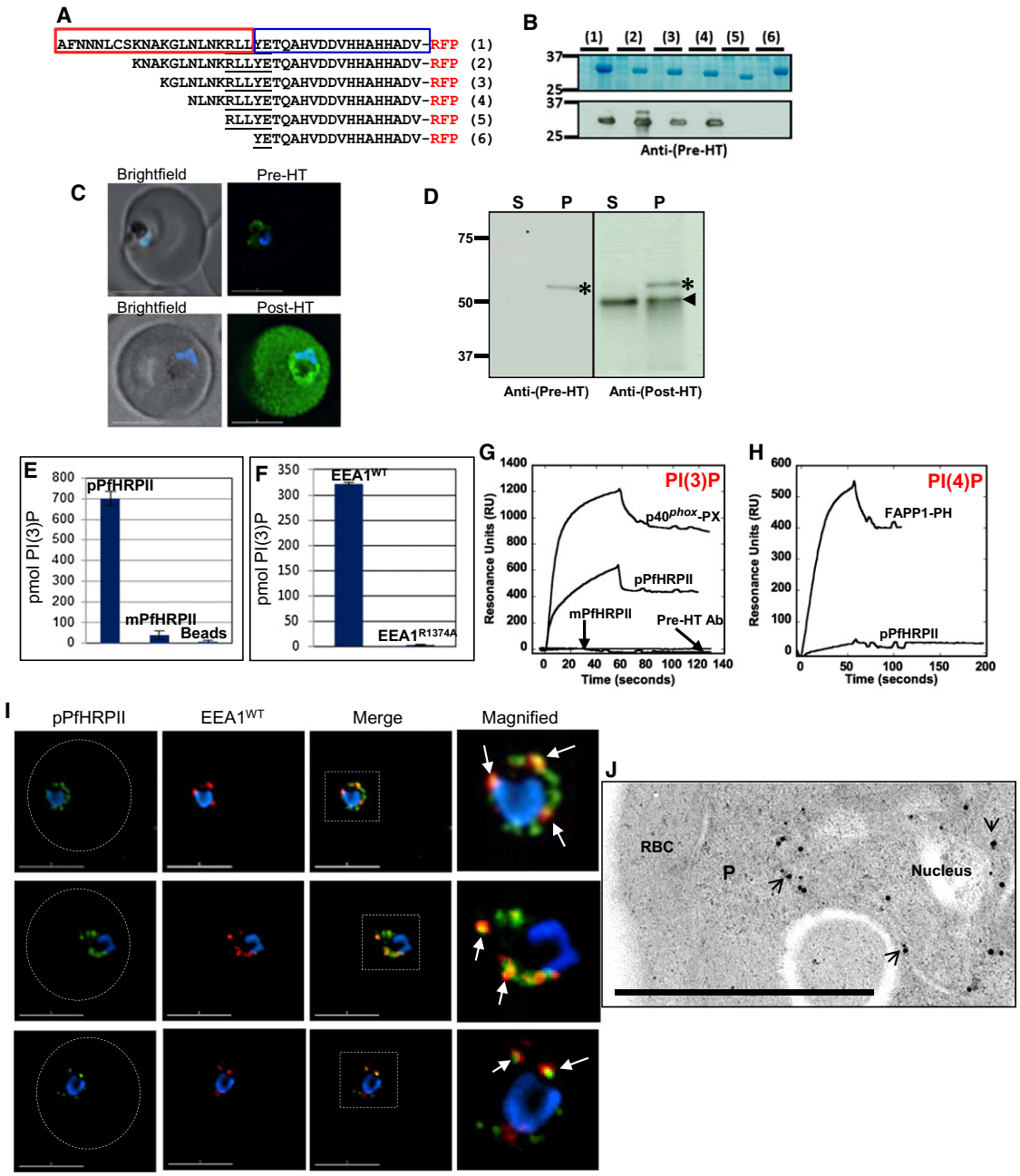

Figure 4. Endogenous HT Signal on Precursor PfHRPII in the ER Associates with PI(3)P Both in Vitro and In Vivo

(A) Sequence of RFP fusions containing the first 40 amino acids present on pPfHRPII, and truncations, used in (B). The pentameric HT core in each sequence is underlined. Peptide regions used to design anti-peptide pre-HT and post-HT antibodies are boxed in red and blue, respectively.

(B) Coomassie-stained gel of paired uninduced and IPTG-induced *E. coli* lysates expressing recombinant N-terminal fusions as indicated in (A) (top) were probed with pre-HT antibody (bottom). Fusions 5 and 6 that lack the pre-HT sequence are not recognized by pre-HT antibody. Molecular weight standards (kDa) are shown.

(C) Pre-HT antibodies recognize a PfHRPII form within the parasite (top). Post-HT antibodies recognize PfHRPII forms in the parasite and erythrocyte (bottom). Nuclei were stained with Hoechst 33342 (blue). Bright-field images, left; fluorescent images, right. Scale bars, 5 μm.

(D) The pre-HT antibody recognizes pPfHRPII as a single protein band slightly above 50 kDa (asterisk in the left panel), present in the pellet (P) fraction of tetanolysin-permeabilized infected erythrocytes but not in the supernatant (S) fraction. Post-HT antibody recognizes a single band at 50 kDa in the supernatant (S) fraction indicating exported and processed, mature HRPII (mPfHRPII). In the P fraction, post-HT antibody recognizes both mPfHRPII (indicated by arrowhead) and pPfHRPII (asterisk in the right panel). Molecular weight standards (kDa) are shown.

(E) Quantitation of PI(3)P bound to pPfHRPII and mPfHRPII. pPfHRPII was immunoprecipitated and the amount of PI(3)P bound was detected by mass ELISA kit. Lysates precleared of pPfHRPII were subjected to immunoprecipitation using post-HT antibodies and PI(3)P amount was determined. To determine nonspecific

N-terminal peptide, suggested cleavage at the AAAA site for both (Figures 5C and 5D), as expected for signal peptidase action. Quantitative analysis of all released peptides confirmed that the efficiency of signal peptide cleavage was comparable for both (Figure 5E and Table S3). Further, intact RQLR containing peptide was recovered from immunopurified Nuk10 protein (Figure 5F). This was observed even with the Nuk10 fraction exported to the erythrocyte (Figures S5A–S5D). These data establish that both the Nuk10-WT and the mutant are released from the ER membrane by signal peptidase and that the oomycete HT motif was not cleaved, likely because it is not a substrate for malarial plasmepsin V. This was unexpected, since cleavage by plasmepsin V was proposed as the export mechanism, yet the oomycete HT signal appears to catalyze export in absence of cleavage. SPR measurements confirm that Nuk10 HT signal bound PI(3)P containing vesicles with 28 nM affinity, whereas the mutant greatly reduced PI(3)P binding (K_d > 2 μM, Figures 5G and S5E), suggesting that PI(3)P binding is the mechanism of export to the host cell.

The principal reason that plasmepsin V is thought to target proteins for export, was the evidence that cleavage of a signal anchor by signal peptidase failed to export protein to the erythrocyte. To further investigate the idea, we engineered an efficient signal peptidase cleavage site (AAAA) in two distinct malaria protein chimeras in which the HT motif was abrogated but the flanking sequences were kept intact (Figure 6). For PfHRPII, we found that mutation of HT signal did not block export of the GFP reporter to the erythrocyte (Figure 6A, middle). However, replacement of all 9 downstream charged residues blocked export (Figure 6A, bottom). Mass spectrometric analysis confirmed all three chimeras were released from the signal anchor either through cleavage of the HT signal or the AAAA signal peptidase site (Figure S6). Hence, the block in export seen in Figure 6A, bottom, is not due to failure to release protein from the membrane. These data suggest that there are HT-independent peptidic signals of parasite protein export to the erythrocyte that may be dependent on charge.

For a second protein, we examined *P. falciparum* erythrocyte membrane protein 3 (PfEMP3), utilized in earlier studies implicating plasmepsin V as the export mechanism (Boddey et al., 2010). As previously reported, replacement of RSLAQ motif with A-AQ abrogated protein export (Figure 6B, top and middle) and resulted in a shift from cleavage by plasmepsin V to cleavage by signal peptidase (Figure S6). However, we show that insertion of the AAAA signal peptidase site followed by replacement of RSLAQ by ASAAA, results in export of GFP to the erythrocyte (Figure 6B, bottom). For this reporter, the primary site for cleavage is within the AAAA sequence, suggesting that it too is recognized by signal peptidase and released from the membrane. Although we do not understand the basis of GFP export in Figures 6A (middle) and 6B (bottom), the data affirm mutations in the HT signal system may shift transport by an HT-independent export pathway. Thus, the earlier conclusion (Boddey et al., 2010) that failure to export in Figure 6B (middle) is due to loss of the HT signal alone may have been premature.

DISCUSSION

The HT signal functions in context of an ~40 amino acid vacuolar translocation signal needed to mediate parasite protein export to the erythrocyte (Hiller et al., 2004; Lopez-Estraño et al., 2003). Thus, the HT signal may be one (likely the most important) region necessary for selective PI(3)P recognition. In malarial HT signals, PI(3)P binding is critically dependent on the high value R in the plasmodial HT logo, providing one of the first clues that lipid binding may play a major role in targeting malaria parasite proteins to the host erythrocyte. The nanomolar affinity displayed by the HT signal of virulence determinants containing the R/KxLxE motif, including the major virulence adhesin PfEMP1, suggests a new mode of PI(3)P binding. Since nanomolar phosphoinositide (PI) binding is primarily attributed to at least four points of contact, it is likely that there are other cationic residues residing in the HT signal and flanking sequences that contribute to PI(3)P recognition. Additionally, hydrophobic residues such as L or others within the HT signal may provide further membrane anchorage through membrane penetration (Lemmon, 2008), whereas the consensus E could form H-bonds with the 5-OH and discriminate against other PIs as previously reported for the FYVE domain (Dumas et al., 2001). Further structural and biophysical studies will be necessary to fully appreciate this novel mechanism of PI(3)P recognition.

The presence of PI(3)P in the malarial ER and its affinity for endogenous HT signals strongly suggests that HT-signal lipid interactions occur early in the ER. Importantly, with the development of specific antibody reagents, we are able to detect ER precursors carrying the HT signal, suggesting that even at steady state a detectable amount of endogenous precursor carrying the HT signal has not been processed by plasmepsin V. Our finding that PI(3)P binding is required for export even when plasmepsin V fails to cleave the oomycete HT signal, leads us to propose that

binding, lysates (without pre-clearing pPfHRPII) were incubated with beads and processed identically. Samples were quantitated using PI(3)P standard curve as shown in Figure S4. Data represents mean ± SEM from triplicates.

(F) Quantitation of PI(3)P bound by the wild-type FYVE domain of EEA1 ($EEA1^{WT}$) and the point mutant ($EEA1^{R1374A}$) in transgenic parasites. The assay was carried out essentially as described in E. Samples were quantitated using PI(3)P standard curve as shown in Figure S4. Data represents mean ± SEM from triplicates.

(G) SPR sensorgrams showing PI(3)P binding for pPfHRPII, mPfHRPII (as described in E); and pre-HT antibody alone. Sensorgrams were also generated for purified p40-phox-PX (226 nM).

(H) SPR sensorgrams of pPfHRPII for PI(4)P. Immunopurified pPfHRPII (as described in E) was used to detect binding to PI(4)P by SPR. Purified FAPP1-PH (1 μM) was used as a control for PI(4)P binding.

(I) Relative distribution of endogenous HT signal in pPfHRPII (green) and $EEA1^{WT}$-mCherry (red) as detected by indirect immunofluorescence assays. Single optical sections of 20 nm thickness are shown. Dotted circles in the left panels indicate red cell membrane. Region within dotted squares are magnified in the right panels. Yellow (and marked by white arrows) indicates sites of $EEA1^{WT}$-mCherry/PI(3)P colocalization with endogenous pPfHRPII (merge). Scale bars, 5 μm.

(J) Immunoelectron micrograph showing sites of colocalization of $EEA1^{WT}$-mCherry/PI(3)P (10 nm gold) with endogenous pPfHRPII (15 nm gold). Arrows show close colocalization of pPfHRPII and $EEA1^{WT}$ in the perinuclear region. Scale bar, 5 μm.

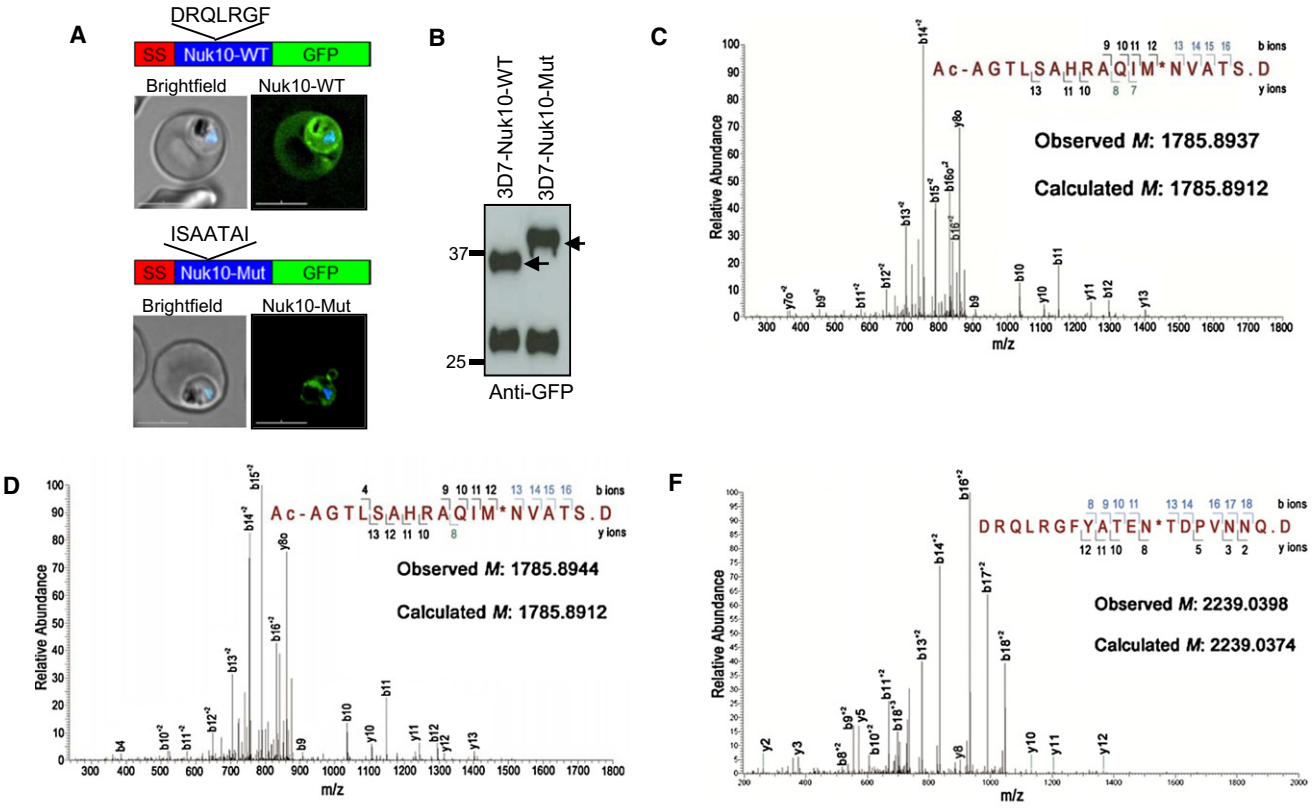

	Nuk10 (WT)-GFP				Nuk10 (Mut)-GFP		
	Peptide	Charge	SC	Area under the curve	Charge	SC	Area under the curve
1	Ac-AGTLSAHR.A	+2	1	5.00E+06	+2	1	3.60E+06
2	Ac-AGTLSAHRA.H	+1, +2	4	2.12E+08	+2	2	1.88E+08
3	Ac-AAGTLSAHRA.H	+2	2	6.44E+07	+2	1	6.13E+07
4	Ac-AAAGTLSAHRA.Q	+2	1	5.49E+06	+2	1	5.31E+06
5	Ac-GTLSAHRAQIM.N	+2	1	1.02E+06	+2	1	1.73E+06
6	Ac-AGTLSAHRAQIM*.N	+2	1	3.36E+06	+2	1	3.26E+06
7	Ac-AGTLSAHRAQIMNVATS.D	+2	1	9.16E+06	+2	2	2.04E+07
8	Ac-AGTLSAHRAQIM*NVATS.D	+2	3	6.21E+07	+2	3	8.32E+07
9	Ac-AAGTLSAHRAQIM*NVATS.D	+2, +3	3	2.48E+07	+2	2	3.32E+07
10	Ac-AAAGTLSAHRAQIM*NVATS.D	ND	ND	ND	+2	1	1.17E+06

Protein-Reporter (HT)	K_d (PI(3)P)
Nuk10 **DRQLRGF-GFP** (RQLR)	28 nM
Nuk10 **ISAATAI-GFP** (SAAT)	> 2 μM

Figure 5. *P. infestans* Nuk10 HT Signal Shows PI(3)P Binding-Dependent Export and Is Not Cleaved by Plasmepsin V

(A) Live *P. falciparum*-infected erythrocytes expressing a secretory chimera of the HT signal of *P. infestans* Nuk10-WT-GFP (top) and corresponding mutant Nuk10-Mut-GFP (bottom). Left, bright-field images with Hoechst 33342 nuclear staining (blue); right, fluorescence images. Scale bars represent 5 μm.

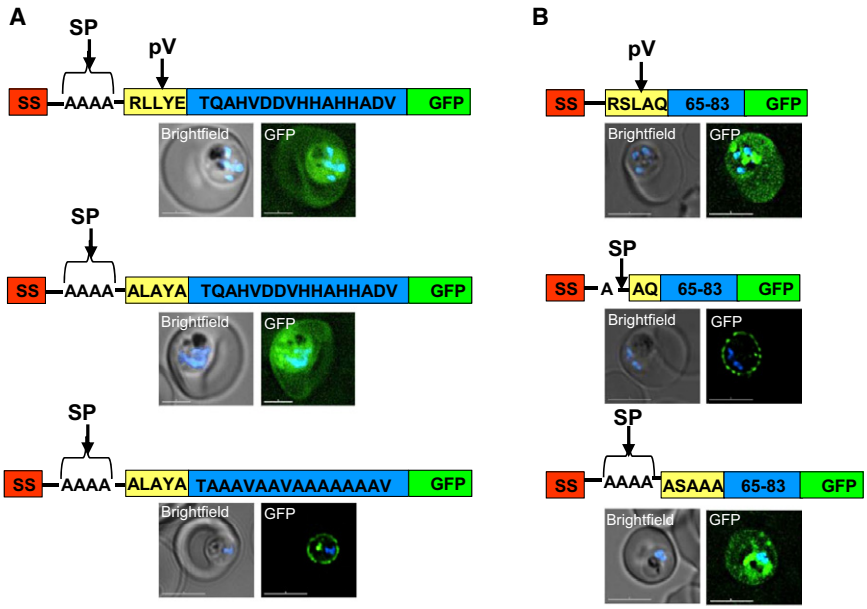

Figure 6. Evidence for HT-Independent Protein Export to the Red Cell

(A) Four alanines were placed between the predicted signal sequence cleavage and the pentameric HT core (RLLYE) or its mutant (ALAYA). In live *P. falciparum*-infected erythrocytes expressing SS-AAAA-HT-GFP, GFP is exported to the red cell (top) and the HT signal (RLLYE) is efficiently cleaved by plasmepsin V (pV; for mass spec analysis of peptides, also see Figure S6). Expression of SS-AAAA-ALAYA-GFP also results in GFP export and cleavage by signal peptidase (SP) at the AAAA site (also see Figure S6). Expression of SS-AAAA-ALAYA-down-GFP with all charge residues downstream of ALAYA replaced with alanine, fails to result in export GFP (bottom), despite cleavage by SP at the AAAA site (also see Figure S6). SP shows heterogeneous cleavage at the AAAA site. Bright-field images with Hoechst 33342 nuclear staining (blue), left; fluorescent images, right. The scale bars represent 5 μm.

(B) Live *P. falciparum*-infected erythrocytes expressing PfEMP3-RSLAQ-GFP exports GFP to the red cell (top), and the HT signal (RSLAQ) is efficiently cleaved by pV (also see Figure S6). PfEMP3xQ-GFP, with modified SP site and lacking HT signal, does not export GFP (center) although it undergoes cleavage by SP at the AQ. However, placement of four alanines (SP cleavage site) upstream of mutated motif in PfEMP3-A4-ASAAA-GFP results in export of GFP and cleavage by SP occurs at AAAA site. SP shows heterogeneous cleavage at the AAAA site. Schematic representation of each construct and cleavage site is shown at the top. Bright-field images also show Hoechst 33342 nuclear staining (blue), and the scale bars represent 5 μm. Also see Figure S6 for detailed LC-MS/MS analyses.

the export mechanism is an efficient, early sorting event in the ER (Figure 7) dependent on high-affinity binding to PI(3)P in the lumen of the ER. When it occurs, HT signal cleavage by plasmepsin V is expected to be restricted to an emerging and/or possibly sealed vesicle. The convergence of amino acid specificity of PI(3)P binding and plasmepsin V cleavage, may suggest that association by PI(3)P may facilitate protease cleavage by plasmepsin V. However cleavage per se (whether by plasmepsin V or signal peptidase) may not provide specificity for host targeting, rather both release protein from the ER membrane.

Our data also suggest that HT-independent export of parasite protein reporters to the host can occur. HT-independent pathways of export have been proposed for major parasite proteins such as *P. falciparum* Skeleton binding protein 1 (PfSBP1) as well as other proteins, which lack the HT signal but that are resident in the secretory structures called Maurer's clefts in the erythrocyte cytoplasm and are thought to promote protein delivery to the host erythrocyte membrane and other destinations in the erythrocyte (Cooke et al., 2006; Spielmann and Gilberger, 2010). Our data suggest that non-HT-dependent

(B) Western blot of Nuk10-WT-GFP and Nuk10-Mut-GFP (indicated by arrows) immunopurified from parasites. Lower bands at ~27 kDa indicate free GFP. Molecular weight standards (in kDa) are shown on the left. The mobility of Nuk10-WT-GFP and Nuk10-Mut-GFP are identical to that seen when these proteins are expressed in *E. coli* indicating that mobility differences are not due to processing by malaria parasites (data not shown).

(C and D) Mass spectrometry analysis of N-terminal peptides, derived from Nuk10-WT-GFP (C) and Nuk10-Mut-GFP (D) chimeras in (A) are shown and indicate that both are cleaved by signal peptidase. Ac- indicates acetylated N terminus and M* indicates dynamic oxidation of Methionine. Observed b and y ions are shown on the peptide sequence and the MS/MS spectra and neutral loss of water is indicated by "o." The +1 ions are shown in black, +2 ions shown in blue and neutral loss of water in green on the peptide sequence. When multiple forms (different charge states or water loss) of an ion were observed, only one form is indicated on the sequence. Observed and calculated M+H masses for (B) and (C) are: peptide B obs. 1785.8937, calc. 1785.8912 (1.4 ppm mass error) and peptide C obs. 1785.8944 and calc. 1785.8912 (1.8 ppm mass error). Also see Figure S5.

(E) Comparison of top ten peptides obtained after AspN digestion and the area under the curve for each shows that signal peptidase processing is equivalent in purified Nuk10-WT-GFP and mutant Nuk10-Mut-GFP. The presence of AAAA at the cleavage site generates heterogeneity at the N terminus, but at levels that are comparable between the two chimeras. Peptides are represented in blue and the acetylated N termini are represented in gray. M* denotes dynamic oxidation of Methionine and Ac- denotes N-terminal acetylation. ND, not detected. Also see Figure S5 and Table S3 for a complete list of peptides.

(F) The HT signal RQLR in Nuk10-WT-GFP chimera is not cleaved by plasmepsin V. Nuk10-WT-GFP was purified from transgenic parasites, digested with AspN and analyzed by LC-MS/MS. Peptide yield of DRQLRGFYATEN*TDPVNNQ.D indicates that plasmepsin V cleavage is not essential for export of Nuk10-WT-GFP. N* denotes deamidation of Asparagine. Observed b and y ions are shown on the peptide and the MS/MS spectra with +1 ions shown in black, +2 ions shown in blue and neutral loss of water in green on the peptide sequence. When multiple forms (different charge states or water loss) of an ion were observed, only one form is indicated on the peptide sequence. Spectrum shown is charge state +3. The observed and calculated masses (M+H) are 2239.0398 and 2239.0374, respectively, with a resulting mass error of 1.1 ppm. Also see Figure S5.

(G) Sequence logo derived from HT signals of *P. infestans* secretory proteins and binding of *P. infestans* Nuk10 HT signal and corresponding mutant to PI(3)P. Amino acids are represented by one-letter abbreviations and color-coded as follows: blue, basic; red, acidic; black, hydrophobic; and green, polar. Height of amino acids indicates their frequency at that position. K_d values of Nuk10-WT and Nuk10 mutant were determined as described in Figure 2D.

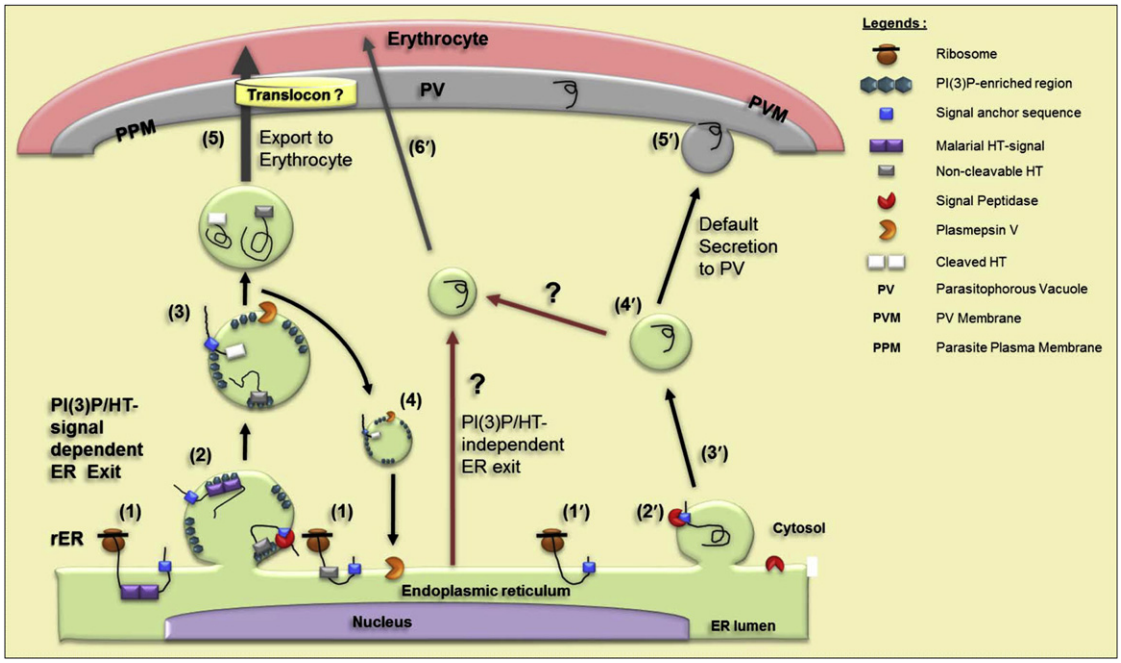

Figure 7. A Model for PI(3)P-Dependent Export from the ER of *P. falciparum*-Infected Erythrocytes

Proteins containing the malarial HT-signal (purple square) or the oomycete HT signal (gray square) are cotranslationally inserted via their signal anchor sequence (blue square) into the ER membrane (step 1). The HT signals recognize the lipid PI(3)P (blue hexagons) enriched in regions of the ER (step 2) and may occur cotranslationally (data not shown). Secretory proteins with a plasmepsin V-refractory HT signal, are cleaved by signal peptidase (red pac-man) but remain associated to PI(3)P. Proteins with the malarial HT signal are cleaved by plasmepsin V (orange pac-man, step 3), which also destroys the PI(3)P binding signal and thus is likely to occur in a newly pinched off vesicle or one whose contents do not freely diffuse with those of the ER. Plasmepsin V and PI(3)P are recycled back to the ER (step 4), whereas cargo targeted to the erythrocyte moves forward across the parasite plasma membrane (PPM), and PVM (step 5). In default secretion, secretory proteins are cotranslationally translocated into the ER (step 1′), the signal sequence (blue square) is cleaved by signal peptidase (red pac-man; steps 2′ and 3′) and protein is delivered through vesicular intermediates to PPM, and released into the PV (steps 4′ and 5′). PI(3)P/HT-independent export to the erythrocyte may reflect a third sorting step in the ER, or later step of transport to PPM (red arrows) before further export (step 6′). Steps 1–5 have ~400 predicted cargo proteins exported to the erythrocyte and thus likely constitute the dominant pathway of protein export to the erythrocyte. The role of the Golgi in these pathways is not known. A translocon has been proposed in export to the erythrocyte, but how it recognizes HT signals lost in the ER is unknown.

export to the erythrocyte is based on charge. Chaperones that interact with charged residues may well distinguish pathways of protein export to the erythrocyte relative to default secretion of well-folded secretory proteins to the PV but these need not be linked to chaperones reported to be associated with plasmepsin V (Goldberg and Cowman, 2010; Russo et al., 2010).

In summary, the parasite likely sorts newly synthesized proteins into two, possibly three, different export pathways that emerge from the ER, thus separating cargo for the erythrocyte from the PV (Figure 7), akin to early models of secretion proposed over a decade ago (Elmendorf and Haldar, 1993; Wiser et al., 1997). Wiser et al. (1997) proposed a "secondary ER" for protein export to the erythrocyte and this was supported by rapid kinetics of secretory protein exit (Crary and Haldar, 1992), but evidence of specialized ER domains in parasite protein export was lacking. The contribution of the Golgi to the PI(3)P/HT-signal ER exit pathway remains unknown. A translocon-mediating export of secretome proteins into the erythrocyte has been proposed (de Koning-Ward et al., 2009). How it recognizes putative protein cargo is unclear, since the HT signal in most plasmodial proteins is largely abrogated in ER exit.

Based on the steady-state distribution of secretory PI(3)P and plasmepsin V, we propose that both recycle back to the ER once HT signal sorting and cleavage are completed (Figure 7), at least in early intraerythrocytic stages called ring and early trophozoite stages investigated in this study. Recent studies have reported the export of a PI3kinase into the erythrocyte and in association with membrane structures in the red cell (Vaid et al., 2010), but how this export occurs and whether PI3kinase is recruited in the secretory pathway is not known. An alternate mechanism for concentration of PI(3)P in the ER could be *trans*-bilayer import of PI(3)P synthesized on the cytoplasmic face. A recent study suggested that blood cell infection increases PI(3)P levels (Tawk et al., 2010), although the overall ratio of PI(3)P in the ER to total cellular PI(3)P is unknown.

The presence of PI(3)P in the lumen of ER regions and its binding to HT signals is consistent with a sorting function for this lipid in malaria parasites. Given that malarial PI(3)P is utilized by the oomycete HT signal to target proteins to the host erythrocyte and malarial signals and oomycete signals are functionally equivalent in both *Plasmodium* and *Phytophthora*, it is possible that PI(3)P also functions in the *P. infestans* ER. Thus, PI(3)P binding in the ER may be a generalized mechanism for

pathogenic secretion in eukaryotic pathogens, aspects of which may be targeted to disrupt pathogen-host interactions that underlie disease.

EXPERIMENTAL PROCEDURES

Plasmid Construction

All the primers used for vector construction are described in the Extended Experimental Procedures and Table S1.

Expression and Purification of Recombinant Proteins in *E. coli*

All recombinant proteins were expressed in *E. coli* BL21 (DE3) cells. His-tagged proteins were purified over Pro-Bond resin (Invitrogen), MBP-tagged proteins were purified over Amylose resin (New England Biolabs), and GST-fusions were purified over Glutathione resin (Clontech). The sequences of recombinant proteins are shown in Table S2. See Extended Experimental Procedures for additional details.

Generation of Antipeptide Antibodies

We used peptides NNLCSKNAKGLNLNKRLL (pre-HT) and YETQAHVDDVHH AHHADV (post-HT), based on sequence N-terminal or C-terminal, respectively, to the deduced plasmepsin V cleavage site of PfHRPII. Rabbit polyclonal antibodies raised to each were designated as anti-(pre-HT) and anti-(post-HT), respectively.

Parasite Culture and Live Cell Imaging

P. falciparum 3D7 parasites and transgenic parasites were propagated in culture in A+ human erythrocytes in RPMI containing Albumax II (GIBCO) and were imaged live in a biological chamber using DeltaVision Deconvolution microscopy (Applied Precision). See Extended Experimental Procedures for additional details.

Immunoprecipitation and Western Blotting of Tagged Transgenic Proteins

P. falciparum parasitized erythrocyte lysates were prepared from cultures at 8%–10% parasitemia. Proteins were extracted and immunopurified using anti-GFP or anti-RFP beads (MBL), separated by SDS-PAGE and either processed for LC-MS/MS or western blotting. See Extended Experimental Procedures for details.

Selective Permeabilization of Infected Erythrocytes

Saponin was used to selectively permeabilize the infected erythrocyte membrane and the PVM (but not the parasite plasma membrane) of *P. falciparum*-infected erythrocytes. For selective permeabilization of just the infected erythrocyte membrane, 100 U of tetanolysin was used. See Extended Experimental Procedures for additional details.

Mass Spectrometry and Peptide Quantitation

Protein bands of interest were excised, digested with AspN and analyzed by LC-MS/MS using reverse phase capillary HPLC with a Thermo Electron LTQ OrbiTrap XL mass spectrometer. The peptide identities of integrated peaks were verified based on retention times of matching MS/MS spectra. See Extended Experimental Procedures for additional details.

Immunolocalization by Indirect Immunofluorescence Assays and Immunoelectron Microscopy

Immunofluorescence arrays (IFAs) were performed on parasites fixed with glutaraldehyde/paraformaldehyde, using indicated primary and secondary antibodies and slides were stained with Hoechst 33342. See Extended Experimental Procedures for additional details.

For immunoelectron microscopy, infected erythrocytes were fixed and embedded in LR white. Thin sections were probed with rabbit anti-mCherry (single labeling) or mouse anti-mCherry and rabbit anti-BiP/ anti-pre-HT, followed by gold conjugated secondary antibodies (10 nm and/or 15 nm). See Extended Experimental Procedures for additional details.

Liposome Pelleting Assay

The liposome sedimentation assays were performed by generating liposomes with POPC, POPE, and/or phosphoinositides. Liposomes were then mixed with proteins to yield solutions containing 1 mM total lipid and 5 μM proteins. Bound proteins were eluted with Laemmli buffer, resolved by SDS-PAGE, and developed with Coomassie dye. See Extended Experimental Procedures for additional details.

SPR Binding Protein-Lipid Interactions

All SPR measurements were performed at 25°C in PBS. Sensor chip surfaces were injected with POPC/POPE/Phosphoinositide (75:20:5) and POPC/POPE (80:20) vesicles at 5 μl/min onto the active surface and the control surface, respectively, to give the same resonance unit (6,000 RU) values. Equilibrium SPR measurements were done at the flow rate of 5 μl/min. Each data set was repeated three times to calculate the mean ± standard deviation. See Extended Experimental Procedures for additional details.

Immunoprecipitation Using Pre-HT and Post-HT Antibodies and Detection of PI(3)P by ELISA

P. falciparum 3D7-infected cells were cultured with 50 μM HIV protease inhibitor Lopinavir (Selleckchem), to inhibit plasmepsin V activity, for 7 hr and cell lysates were subjected to immunoprecipitation. The relative amounts of pPfHRPII (immunoprecipitated by pre-HT antibodies) and mPfHRPII (immunoprecipitated by post-HT antibodies) were determined by western blotting with a mouse anti-PfHRPII and densitometry (data not shown). Equal amounts of pPfHRPII and mPfHRPII were used to detect PI(3)P binding by SPR and estimate bound cellular PI(3)P. See Extended Experimental Procedures for additional details.

SUPPLEMENTAL INFORMATION

Supplementation Information includes Extended Experimental Procedures, six figures, and three tables and can be found with this article online at doi:10.1016/j.cell.2011.10.051.

ACKNOWLEDGMENTS

This project was conceived by K.H., R.V.S., and S.B., and the experiments were planned by K.H., R.V.S., S.B., D.W.S., and K.D.S. S.B., R.V.S., and K.D.S. conducted the experiments. K.H., R.V.S., and S.B. wrote the paper with input from all authors. We thank Yi Xue and Jordan L. Scott for excellent technical assistance, Andrew Osborne (University College of London) for helpful discussions, and Caroline Furtado Junqueira for help in figure representation. We would also like to thank Lennell Reynolds Jr., the Cell Imaging Facility at Northwestern University, and William Archer at the University of Notre Dame for help with electron microscopy. This work was partially supported by NIH grants HL069630, AI039071, HL078826 (K.H.); AI081077 (R.V.S.); HL038794 (D.W.S.) and CA10815 (Wistar Proteomics Core Facility).

Received: June 30, 2011
Revised: September 11, 2011
Accepted: October 28, 2011
Published: January 19, 2012

REFERENCES

Bhattacharjee, S., Hiller, N.L., Liolios, K., Win, J., Kanneganti, T.D., Young, C., Kamoun, S., and Haldar, K. (2006). The malarial host-targeting signal is conserved in the Irish potato famine pathogen. PLoS Pathog. *2*, e50.

Boddey, J.A., Hodder, A.N., Günther, S., Gilson, P.R., Patsiouras, H., Kapp, E.A., Pearce, J.A., de Koning-Ward, T.F., Simpson, R.J., Crabb, B.S., and Cowman, A.F. (2010). An aspartyl protease directs malaria effector proteins to the host cell. Nature *463*, 627–631.

Chang, H.H., Falick, A.M., Carlton, P.M., Sedat, J.W., DeRisi, J.L., and Marletta, M.A. (2008). N-terminal processing of proteins exported by malaria parasites. Mol. Biochem. Parasitol. *160*, 107–115.

Cooke, B.M., Buckingham, D.W., Glenister, F.K., Fernandez, K.M., Bannister, L.H., Marti, M., Mohandas, N., and Coppel, R.L. (2006). A Maurer's cleft-associated protein is essential for expression of the major malaria virulence antigen on the surface of infected red blood cells. J. Cell Biol. *172*, 899–908.

Crary, J.L., and Haldar, K. (1992). Brefeldin A inhibits protein secretion and parasite maturation in the ring stage of Plasmodium falciparum. Mol. Biochem. Parasitol. *53*, 185–192.

de Koning-Ward, T.F., Gilson, P.R., Boddey, J.A., Rug, M., Smith, B.J., Papenfuss, A.T., Sanders, P.R., Lundie, R.J., Maier, A.G., Cowman, A.F., and Crabb, B.S. (2009). A newly discovered protein export machine in malaria parasites. Nature *459*, 945–949.

Dou, D., Kale, S.D., Wang, X., Jiang, R.H., Bruce, N.A., Arredondo, F.D., Zhang, X., and Tyler, B.M. (2008). RXLR-mediated entry of Phytophthora sojae effector Avr1b into soybean cells does not require pathogen-encoded machinery. Plant Cell *20*, 1930–1947.

Duffy, P.E., and Fried, M. (2003). Plasmodium falciparum adhesion in the placenta. Curr. Opin. Microbiol. *6*, 371–376.

Dumas, J.J., Merithew, E., Sudharshan, E., Rajamani, D., Hayes, S., Lawe, D., Corvera, S., and Lambright, D.G. (2001). Multivalent endosome targeting by homodimeric EEA1. Mol. Cell *8*, 947–958.

Elmendorf, H.G., and Haldar, K. (1993). Secretory transport in Plasmodium. Parasitol. Today (Regul. Ed.) *9*, 98–102.

Goldberg, D.E., and Cowman, A.F. (2010). Moving in and renovating: exporting proteins from Plasmodium into host erythrocytes. Nature Rev. *8*, 617–621.

Haldar, K., and Mohandas, N. (2007). Erythrocyte remodeling by malaria parasites. Curr. Opin. Hematol. *14*, 203–209.

Hiller, N.L., Bhattacharjee, S., van Ooij, C., Liolios, K., Harrison, T., Lopez-Estraño, C., and Haldar, K. (2004). A host-targeting signal in virulence proteins reveals a secretome in malarial infection. Science *306*, 1934–1937.

Kale, S.D., Gu, B., Capelluto, D.G., Dou, D., Feldman, E., Rumore, A., Arredondo, F.D., Hanlon, R., Fudal, I., Rouxel, T., et al. (2010). External lipid PI3P mediates entry of eukaryotic pathogen effectors into plant and animal host cells. Cell *142*, 284–295.

Kutateladze, T.G. (2010). Translation of the phosphoinositide code by PI effectors. Nat. Chem. Biol. *6*, 507–513.

Kyes, S.A., Kraemer, S.M., and Smith, J.D. (2007). Antigenic variation in Plasmodium falciparum: gene organization and regulation of the var multigene family. Eukaryot. Cell *6*, 1511–1520.

Lee, S.A., Eyeson, R., Cheever, M.L., Geng, J., Verkhusha, V.V., Burd, C., Overduin, M., and Kutateladze, T.G. (2005). Targeting of the FYVE domain to endosomal membranes is regulated by a histidine switch. Proc. Natl. Acad. Sci. USA *102*, 13052–13057.

Lemmon, M.A. (2008). Membrane recognition by phospholipid-binding domains. Nat. Rev. Mol. Cell Biol. *9*, 99–111.

Lopez-Estraño, C., Bhattacharjee, S., Harrison, T., and Haldar, K. (2003). Cooperative domains define a unique host cell-targeting signal in Plasmodium falciparum-infected erythrocytes. Proc. Natl. Acad. Sci. USA *100*, 12402–12407.

Maier, A.G., Cooke, B.M., Cowman, A.F., and Tilley, L. (2009). Malaria parasite proteins that remodel the host erythrocyte. Nature Rev. *7*, 341–354.

Marti, M., Good, R.T., Rug, M., Knuepfer, E., and Cowman, A.F. (2004). Targeting malaria virulence and remodeling proteins to the host erythrocyte. Science *306*, 1930–1933.

McLaughlin, S., Wang, J., Gambhir, A., and Murray, D. (2002). PIP(2) and proteins: interactions, organization, and information flow. Annu. Rev. Biophys. Biomol. Struct. *31*, 151–175.

Miller, L.H., Baruch, D.I., Marsh, K., and Doumbo, O.K. (2002). The pathogenic basis of malaria. Nature *415*, 673–679.

Nguitragool, W., Bokhari, A.A., Pillai, A.D., Rayavara, K., Sharma, P., Turpin, B., Aravind, L., and Desai, S.A. (2011). Malaria parasite clag3 genes determine channel-mediated nutrient uptake by infected red blood cells. Cell *145*, 665–677.

Osborne, A.R., Speicher, K.D., Tamez, P.A., Bhattacharjee, S., Speicher, D.W., and Haldar, K. (2010). The host targeting motif in exported Plasmodium proteins is cleaved in the parasite endoplasmic reticulum. Mol. Biochem. Parasitol. *171*, 25–31.

Russo, I., Babbitt, S., Muralidharan, V., Butler, T., Oksman, A., and Goldberg, D.E. (2010). Plasmepsin V licenses Plasmodium proteins for export into the host erythrocyte. Nature *463*, 632–636.

Sargeant, T.J., Marti, M., Caler, E., Carlton, J.M., Simpson, K., Speed, T.P., and Cowman, A.F. (2006). Lineage-specific expansion of proteins exported to erythrocytes in malaria parasites. Genome Biol. *7*, R12.

Spielmann, T., and Gilberger, T.W. (2010). Protein export in malaria parasites: do multiple export motifs add up to multiple export pathways? Trends Parasitol. *26*, 6–10.

Stace, C.L., and Ktistakis, N.T. (2006). Phosphatidic acid- and phosphatidylserine-binding proteins. Biochim. Biophys. Acta *1761*, 913–926.

Tawk, L., Chicanne, G., Dubremetz, J., Richard, V., Payrastre, B., Vial, H.J., Roy, C., and Wengelnik, K. (2010). Phosphatidylinositol 3-phosphate, an essential lipid in plasmodium, localizes to the food vacuole membrane and the apicoplast. Eukaryot. Cell *9*, 1519–1530.

Vaid, A., Ranjan, R., Smythe, W.A., Hoppe, H.C., and Sharma, P. (2010). PfPI3K, a phosphatidylinositol-3 kinase from Plasmodium falciparum, is exported to the host erythrocyte and is involved in hemoglobin trafficking. Blood *115*, 2500–2507.

van Ooij, C., Tamez, P., Bhattacharjee, S., Hiller, N.L., Harrison, T., Liolios, K., Kooij, T., Ramesar, J., Balu, B., Adams, J., et al. (2008). The malaria secretome: from algorithms to essential function in blood stage infection. PLoS Pathog. *4*, e1000084.

Whisson, S.C., Boevink, P.C., Moleleki, L., Avrova, A.O., Morales, J.G., Gilroy, E.M., Armstrong, M.R., Grouffaud, S., van West, P., Chapman, S., et al. (2007). A translocation signal for delivery of oomycete effector proteins into host plant cells. Nature *450*, 115–118.

World Health Organization (2010). MalariaReport, http://www.who.int/malaria/world_malaria_report_2010.

Wiser, M.F., Lanners, H.N., Bafford, R.A., and Favaloro, J.M. (1997). A novel alternate secretory pathway for the export of *Plasmodium* proteins into the host erythrocyte. Proc. Natl. Acad. Sci. USA *94*, 9108–9113.